NACA RM L8L31

NACA

RESEARCH MEMORANDUM

THEORETICAL INVESTIGATION OF THE DYNAMIC LATERAL STABILITY CHARACTERISTICS OF DOUGLAS DESIGN NO. 39C, AN EARLY VERSION OF THE X-3 RESEARCH AIRPLANE

By Charles V. Bennett

Langley Aeronautical Laboratory
Langley Air Force Base, Va.

NATIONAL ADVISORY COMMITTEE
FOR AERONAUTICS

WASHINGTON

January 18, 1949

NATIONAL ADVISORY COMMITTEE FOR AERONAUTICS

RESEARCH MEMORANDUM

THEORETICAL INVESTIGATION OF THE DYNAMIC LATERAL STABILITY CHARACTERISTICS OF DOUGLAS DESIGN NO. 39C, AN EARLY VERSION OF THE X-3 RESEARCH AIRPLANE

By Charles V. Bennett

SUMMARY

As a part of a study of the theoretical dynamic lateral stability characteristics of several high-speed research airplanes, calculations have been made of the lateral stability of Douglas design No. 39C, an early version of the X-3 research airplane.

Calculations were made for the airplane at Mach numbers of 0.75 and 2.3 and for the landing condition. The results indicate that the lateral oscillation would be stable for the $M = 0.75$ condition and for the landing condition and could be made stable for the $M = 2.3$ condition by increasing the vertical-tail area. Only the landing condition would satisfy the U. S. Air Force requirement for damping of the lateral oscillation. The spiral mode would be slightly unstable for the $M = 0.75$ condition and the landing condition but would be well within the Air Force requirement. The calculated motions indicated the predominant motion was rolling regardless of the type of disturbance.

The oscillatory stability was most sensitive to the damping-in-roll parameter and to the inclination of the principal axis of inertia. Increasing the damping in roll increased the oscillatory stability for the landing condition but decreased the stability for the $M = 2.3$ condition.

INTRODUCTION

A study of the theoretical dynamic lateral stability characteristics of several high-speed research airplanes is being made by the Stability Research Division of the Langley Laboratory. As a part of this study, lateral-stability calculations were made for the Douglas design No. 39C,

an early version of the X-3 research airplane shown in the sketch of figure 1. The calculations were based on the values of mass and aerodynamic parameters presented in table I for this particular design. The mass parameters were supplied by the Douglas Aircraft Company. The aerodynamic parameters are based on the external dimensions given by the company. The calculations were made on the relay computer at the Langley Laboratory, and the results were analyzed in the Langley free-flight-tunnel section. The results of the calculations are presented herein in the form of oscillatory-stability boundaries, period and time to damp to one-half amplitude of the oscillations, and the motions of the airplane resulting from a disturbance in yaw or roll.

Calculations of the lateral stability of design No. 39C have also been made by the Douglas Company and are presented in references 1 and 2. Some of the aerodynamic parameters that were used for the calculations of references 1 and 2 are not in good agreement with those of the present investigation.

SYMBOLS AND COEFFICIENTS

S	wing area, square feet
$\bar{c}$	mean aerodynamic chord, feet
V	airspeed, feet per second
b	wing span, feet
q	dynamic pressure, pounds per square foot
ρ	air density, slugs per cubic foot
W	weight, pounds
g	acceleration of gravity, feet per second per second
m	mass, slugs (W/g)
μ_b	relative density factor based on wing span $(m/\rho Sb)$
α	angle of attack of reference axis (fig. 1), degrees
η	angle of attack of principal longitudinal axis of airplane, positive when principal axis is above flight path at the nose, degrees

ϵ angle between reference axis and principal axis, positive when reference axis is above principal axis at the nose, degrees

θ angle between reference axis and horizontal axis, positive when reference axis is above horizontal axis at the nose, degrees

γ angle of flight to horizontal axis, positive in a climb, degrees

ψ angle of azimuth measured from original flight direction, degrees except in equations of motion, per radian

β angle of sideslip, degrees except in equations of motion, per radian

ϕ angle of bank, degrees except in equations of motion, per radian

R Routh's discriminant ($R = BCD - AD^2 - B^2E$ where A, B, C, D, and E are constants representing coefficients of the lateral stability equation)

k_{X_o} radius of gyration about principal longitudinal axis, feet

k_{Z_o} radius of gyration about principal vertical axis, feet

K_{X_o} nondimensional radius of gyration about principal longitudinal axis $\left(k_{X_o}/b\right)$

K_{Z_o} nondimensional radius of gyration about principal vertical axis $\left(k_{Z_o}/b\right)$

K_X nondimensional radius of gyration about longitudinal stability axis $\left(\sqrt{K_{X_o}^2 \cos^2 \eta + K_{Z_o}^2 \sin^2 \eta}\right)$

K_Z nondimensional radius of gyration about vertical stability axis $\left(\sqrt{K_{Z_o}^2 \cos^2 \eta + K_{X_o}^2 \sin^2 \eta}\right)$

K_{XZ} nondimensional product-of-inertia parameter $\left[\left(K_{Z_o}^2 - K_{X_o}^2\right)\cos \eta \sin \eta\right]$

C_L lift coefficient (Lift/qS)

C_n yawing-moment coefficient (Yawing moment/qSb)

C_l rolling-moment coefficient (Rolling moment/qSb)

C_Y lateral-force coefficient (Lateral force/qS)

C_{Y_β} rate of change of lateral-force coefficient with angle of sideslip, per radian $\left(\partial C_Y/\partial\beta\right)$

C_{n_β} rate of change of yawing-moment coefficient with angle of sideslip, per degree except in equations of motion, per radian $\left(\partial C_n/\partial\beta\right)$

C_{l_β} rate of change of rolling-moment coefficient with angle of sideslip, per degree except in equations of motion, per radian $\left(\partial C_l/\partial\beta\right)$

C_{Y_p} rate of change of lateral-force coefficient with rolling-angular-velocity factor, per radian $\left(\dfrac{\partial C_Y}{\partial\frac{pb}{2V}}\right)$

C_{l_p} rate of change of rolling-moment coefficient with rolling-angular-velocity factor, per radian $\left(\dfrac{\partial C_l}{\partial\frac{pb}{2V}}\right)$

C_{n_p} rate of change of yawing-moment coefficient with rolling-angular-velocity factor, per radian $\left(\dfrac{\partial C_n}{\partial\frac{pb}{2V}}\right)$

C_{l_r} rate of change of rolling-moment coefficient with yawing-angular-velocity factor, per radian $\left(\dfrac{\partial C_l}{\partial\frac{rb}{2V}}\right)$

C_{n_r} rate of change of yawing-moment coefficient with yawing-angular-velocity factor, per radian $\left(\dfrac{\partial C_n}{\partial\frac{rb}{2V}}\right)$

C_{Y_r} rate of change of lateral-force coefficient with yawing-angular-velocity factor, per radian $\left(\frac{\partial C_Y}{\partial \frac{rb}{2V}}\right)$

l tail length (distance from center of gravity to rudder hinge line), feet

$\bar{z}$ height of center of pressure of vertical tail above fuselage axis, feet

p rolling-angular velocity, radians per second

r yawing-angular velocity, radians per second

D_b differential operator $\left(\frac{d}{ds_b}\right)$

s_b distance along flight path, spans (Vt/b)

λ complex root of stability equation $(c \pm id)$

t time, seconds

P period of oscillation, seconds

$T_{1/2}$ time for amplitude of oscillation to change by factor of 2 (positive value indicates a decrease to half amplitude, negative value indicates an increase to double amplitude)

$C_{1/2}$ cycles for amplitude of oscillation to change by factor of 2 (positive value indicates a decrease to half amplitude, negative value indicates an increase to double amplitude)

EQUATIONS OF MOTION

The nondimensional lateral equations of motion, referred to the stability-axes system of figure 2, are:

Roll

$$2\mu_b \left(K_X^2 D_b^2 \phi + K_{XZ} D_b^2 \psi\right) = C_{l_\beta} \beta + \frac{1}{2} C_{l_p} D_b \phi + \frac{1}{2} C_{l_r} D_b \psi$$

Yaw

$$2\mu_b \left(K_Z^2 D_b^2 \psi + K_{XZ} D_b^2 \phi\right) = C_{n_\beta} \beta + \frac{1}{2} C_{n_p} D_b \phi + \frac{1}{2} C_{n_r} D_b \psi$$

Sideslip

$$2\mu_b \left(D_b \beta + D_b \psi\right) = C_{Y_\beta} \beta + \frac{1}{2} C_{Y_p} D_b \phi + C_L \phi + \frac{1}{2} C_{Y_r} D_b \psi + \left(C_L \tan \gamma\right) \psi$$

When $\phi_o e^{\lambda s_b}$ is substituted for ϕ, $\psi_o e^{\lambda s_b}$ for ψ, and $\beta_o e^{\lambda s_b}$ for β in the equations written in determinant form, λ must be a root of the stability equation

$$A\lambda^4 + B\lambda^3 + C\lambda^2 + D\lambda + E = 0$$

where A, B, C, D, and E are functions of the coefficients of the mass and aerodynamic parameters as given in reference 3.

The conditions for neutral oscillatory stability as shown by reference 4 are that the coefficients of the stability equation satisfy Routh's discriminant set equal to zero

$$R = BCD - AD^2 - B^2E = 0$$

and that the coefficients B and D have the same sign. In general, the sign of the coefficient B is determined by the factors $-C_{Y_\beta}$, $-C_{n_r}$, and $-C_{l_p}$ which appear in the predominant terms of B. Thus, B is positive in the usual case if there is positive weathercock stability and positive damping in roll.

CALCULATIONS

Calculations were made to determine the neutral-oscillatory-stability boundaries, the period and time to damp to one-half amplitude of the

lateral oscillations, and the motions resulting from a disturbance in yaw or roll for three conditions as follows:

Condition	Mach number	Altitude (feet)	C_L
I	0.75	35,000	0.50
II	2.3	35,000	.05
III	.206	0	1.20

The aerodynamic and mass characteristics used in the calculations for the three conditions are presented in table I. Values of some of the basic stability parameters were obtained from tests in the Langley free-flight tunnel of a model which was very similar to a $\frac{1}{10}$-scale model of the X-3 research airplane. The results of these tests are presented in reference 5. The parameters that were not available from tests were estimated from the charts of reference 6. The method of reference 7 was used to determine the tail contributions to the parameters C_{n_p}, C_{l_p}, C_{n_r}, and C_{l_r}. The aerodynamic parameters for Mach number 2.3 (condition II) were estimated from the formulas of reference 8.

Because the parameters C_{l_p}, C_{n_p}, C_{l_r}, C_{n_r}, and η were estimated, additional oscillatory-stability boundaries were calculated for conditions II and III with each of these parameters varied by 50 and 150 percent to indicate what would be the effect on stability of inaccurate estimations of these parameters.

The period and time to damp to one-half amplitude in seconds as given by the equations,

$$T_{1/2} = \frac{-0.69}{c} \frac{b}{V}$$

$$P = \frac{2\pi}{d} \frac{b}{V}$$

and

$$C_{1/2} = T_{1/2} \Big/ P$$

where c and d are the real and imaginary parts of the complex root of the stability equation, were calculated for the three conditions. The combinations of C_{n_β} and C_{l_β} that were obtained from force tests of a model similar to the X-3 (reference 5) were used for conditions I and III, and the combination of C_{n_β} and C_{l_β} given in references 1 and 2 was used for condition II. In references 1 and 2 it was shown that an increase in the vertical-tail area from 25 square feet to 35 square feet was necessary to make the airplane stable. Calculations, therefore were made in the present investigation for condition II (assumed to be critical because of the high speed) with values of C_{n_β} and C_{l_β} for both the 25 and 35 square feet vertical tails as were given in references 1 and 2. It is pointed out, however, that the low-speed data on a model similar to the X-3 (reference 5) indicated that the airplane with the 25 square feet vertical tail would have considerably more directional stability than was assumed in references 1 and 2. It is believed, therefore, that an increase in vertical-tail area to 35 square feet might not be necessary to obtain the higher values of C_{n_β} indicated as necessary in references 1 and 2.

Calculations were also made to determine the motions of the airplane resulting from a disturbance in roll or yaw ($C_l = 0.01$ or $C_n = 0.01$) which was removed after 0.15 second. The magnitude of the disturbance was arbitrarily selected and may not be typical of control or gust disturbances which would be experienced on the airplane. However, the motion for any other arbitrary magnitude of the disturbance can be simply determined since the motion is proportional to the disturbance.

RESULTS AND DISCUSSION

Neutral-Oscillatory-Stability Boundaries and Period and Time To Damp to One-Half Amplitude of the Oscillatory Mode

The results of calculations of the neutral-oscillatory-stability boundaries are shown in figures 3 to 6 for conditions I, II, and III. The assumed values of C_{n_β} and C_{l_β} of the airplane for the three conditions are shown in these figures and the period and time to damp to one-half amplitude for each condition are also indicated. The period and time to damp for all airplane conditions are summarized in table II.

The Air Force requirement for damping of a lateral oscillation is shown in figure 7. This requirement specifies the minimum amount of

damping as a function of the period which would be considered satisfactory. This Air Force requirement is stricter than that used in the past (oscillation must damp to one-half amplitude in 2 cycles or less) in the range of periods from 1 to 4 seconds. Therefore, the oscillatory stability of the X-3 airplane as calculated and presented herein is discussed in terms of this requirement. It should be noted that the reciprocal of $T_{1/2}$ has been plotted as the ordinate in figure 7 so that increased stability is shown by the larger values of the ordinate.

Condition I.- The oscillatory-stability boundaries for condition I are shown in figure 3. The stable and unstable regions which by definition are separated by the $R = 0$ boundary were determined by calculating the periods and time to damp to one-half amplitude for the points A, B, C, and D shown in figure 3. The results of these calculations are shown in figure 4, but are principally of academic interest because of the large negative-dihedral range which is involved in this particular case. Figure 4 shows that upon crossing over one of the branches of the $R = 0$ boundary from point A to point B, the long-period oscillation became unstable. From point B to point C, the period was reduced from 23 seconds to 6 seconds and at point C the oscillation was still unstable. No further calculations were made between these points to determine whether the period of the oscillation changed abruptly or whether there was some position where both a short-period and long-period oscillation would appear. When the other branch of the $R = 0$ boundary was crossed (point C to D), the oscillation became stable and the period was further reduced. Thus, these calculations show that the oscillatorily unstable region is located between the two branches of the $R = 0$ boundary (fig. 3).

The location of the boundaries in the second quadrant (fig. 3) with the stable region to the right of the short-period boundary indicates that the airplane would be oscillatorily stable for this condition where $C_{n_\beta} = 0.006$ and $C_{l_\beta} = -0.002$. These values of C_{n_β} and C_{l_β} for the airplane were obtained from reference 5 and correspond to a vertical-tail area of 25 square feet.

The amount of oscillatory stability for the airplane (with the values of C_{n_β} and C_{l_β} of 0.006 and -0.002), which is shown by P and $T_{1/2}$ in figure 3 and in table II, is only slightly below the minimum which is required by the Air Force for satisfactory damping of the oscillation as shown in figure 7.

Condition II.- The oscillatory stability boundary for the airplane flight condition II is shown in figure 5 to be located in the first quadrant of the C_{n_β}, C_{l_β} plane. In this case only the one branch

of $R = 0$ shown is a valid oscillatory-stability boundary. From this figure it may be seen that for the airplane to be on the stable side of the boundary, it must have low effective dihedral and high directional stability. The two symbols shown on this figure represent the airplane with two combinations of C_{n_β} and C_{l_β}: $C_{n_\beta} = 0.0022$, $C_{l_\beta} = -0.0014$ which according to references 1 and 2 represent the airplane for this condition with the small (25 sq ft) vertical tail, and $C_{n_\beta} = 0.0047$, $C_{l_\beta} = -0.0024$ which represents the airplane with the 35 square foot vertical tail. The airplane moves from the unstable to the stable region of figure 5 when the vertical-tail area is increased from 25 to 35 square feet. Again, it is pointed out that on a basis of the tests reported in reference 5 these values are probably lower than those that will be obtained for the airplane and the airplane might possible be in the stable region even with the 25 square foot vertical tail.

The period and time to damp to one-half amplitude of the lateral oscillation for these combinations of C_{n_β} and C_{l_β} are shown in figure 5 and in table II. These data indicate the period was reduced from 2.04 seconds to 1.4 seconds and that the time of 5.24 seconds to double amplitude was changed to 8.39 seconds to halve amplitude when the tail area was increased from 25 to 35 square feet. However, the damping is not sufficient even for the larger tail area to meet the Air Force requirement shown in figure 7.

Condition III.- The $R = 0$ boundary for condition III is shown in figure 6. This boundary is located in the fourth quadrant of the C_{n_β}, C_{l_β} plane and indicates that for the values of C_{n_β} and C_{l_β} assumed for the airplane in condition III $\left(C_{n_\beta} = 0.0096;\ C_{l_\beta} = -0.00275\right)$ the airplane would be oscillatorily stable.

The landing condition meets the Air Force requirement for satisfactory damping of the lateral oscillation as shown in figure 7; whereas, the other two conditions for which calculations were made did not meet the requirement.

Effect of varying C_{l_p}.- The effect on the oscillatory-stability boundaries of increasing or decreasing C_{l_p} by 50 percent for conditions II and III is shown in figure 8. These results indicate that an increase in the damping-in-roll parameter $-C_{l_p}$ increased the stability for condition III but decreased the stability for condition II. The trend shown for condition III was shown in reference 9 and is

considered typical, but the opposite trend for condition II can be explained by examining the simplified expressions for $R = 0$ in reference 3. It is obvious that the oscillatory boundary is not a function of any one mass or aerodynamic parameter but is a function of combinations of these parameters for any one condition. The simplified expressions for $R = 0$, presented in reference 3, offer a simple means of noting the effects of varying these parameters. The combination of mass and aerodynamic parameters are such for condition II that an increase in the damping-in-roll parameter decreased the oscillatory stability. The factor believed mainly responsible for this unusual trend is the term $C_{n_p} - 2C_L K_Z^2$ which has an important bearing on the $R = 0$ boundary. The individual values of C_{n_p} (positive for condition II and negative for condition III) and the value of K_Z^2 (which is a function of the inclination of the principal axis and which is positive for condition II and negative for condition III) are responsible for the sign of the term being minus for condition III and positive for condition II. When these particular values for condition II were substituted into the simplified equations, it was found that the stability would be expected to decrease when C_{l_p} was increased.

The unusual looking boundary that was obtained for condition II, when the damping in roll was decreased, is the same boundary that was shown in figure 12 of reference 3. This was discussed in detail in reference 3, which showed that the boundary was a short-period boundary for values of C_{l_β} up to approximately -0.006 where it transforms into a long-period oscillatory boundary.

Effect of varying C_{n_p}.- The effect on the oscillatory-stability boundaries of increasing or decreasing C_{n_p} by 50 percent is shown in figure 9 for conditions II and III. These results indicate that a positive increase in C_{n_p} for either condition would increase the range for stability. An error of 50 percent would not appreciably affect the calculated stability of condition III because the boundary is located well away from the actual airplane condition, but an error of 50 percent might greatly affect the calculated stability of the airplane for condition II where the boundary is much closer to the airplane condition.

Effect of varying C_{n_r}.- The effect of varying C_{n_r} for conditions II and III is shown in figure 10. These data indicate that

increasing C_{n_r} in the negative direction for condition II resulted in a slight stabilizing shift in the boundary. A 50-percent increase or decrease in C_{n_r} had no effect on the $R = 0$ boundary for condition III.

Effect of varying C_{l_r}.- The effect of varying C_{l_r} for conditions II and III is shown in figure 11. These data indicate no appreciable shift in the $R = 0$ boundary for either condition when C_{l_r} was increased or decreased by 50 percent.

Effect of principal axis inclination.- The effect on the oscillatory boundary of varying the inclination of the principal axis of inertia for condition II is shown in figure 12. The results of these calculations indicate a destabilizing shift of the $R = 0$ boundary when η was changed from the basic value of -2° to -4° and a large stabilizing effect when it was changed to 0°. This effect has been studied in other NACA investigations and in references 1 and 2 where the same trend was noted.

In order to help determine the meaning of the large shift in the $R = 0$ boundary for condition II when η was changed to 0°, both the short and long-period branches of this boundary have been replotted in figure 13. The period and time to damp to one-half amplitude were calculated for several values of C_{l_β} across the boundaries for $C_{n_\beta} = 0.004$. The data on this figure show that crossing the short-period branch of the boundary from point A to point B results in the short-period oscillation becoming stable. The short-period oscillation becomes progressively more stable with increasing $-C_{l_\beta}$. A long-period oscillation appears and is unstable as the long-period branch is crossed (point E). There is little or no practical significance to the long-period boundary in this particular case in that it appears at very large values of $-C_{l_\beta}$ (corresponding to more than 60° effective dihedral) which would be well beyond the range in which the airplane would operate.

Aperiodic modes.- The two aperiodic modes (damping-in-roll mode and spiral mode) for the airplane conditions I, II, and III are given in table II. For all conditions the damping-in-roll mode is very stable. The spiral mode is unstable for conditions I and III but requires 304 seconds and 64 seconds respectively to double amplitude. The Air Force criterion states that the spiral mode need not be stable, but if it is unstable it should not double in less than 4 seconds. This requirement is satisfied for all conditions investigated.

The calculations of the oscillatory-stability boundaries presented herein are in qualitative agreement with the calculations that were presented in references 1 and 2 even though some of the parameters used were not in agreement with those of references 1 and 2.

Motions Following Disturbances

The motions resulting from a disturbance in yaw or roll are shown in figures 14, 15, and 16 for conditions I, II, and III. The predominant motion as shown on these figures is the rolling motion regardless of the type of disturbance. The predominant rolling motion is probably caused by the high values of $-C_{l_\beta}$, the low damping in roll, and the low rolling inertia. Of course, the high directional stability would limit the sideslip angle β, but the rolling moment was great even for small angles of sideslip. The angles of bank that were reached for the high-speed condition II were approximately 10 times the angles that were reached for conditions I and III. The large angle of bank encountered for condition II results from the very high airspeed.

In addition to calculating the motions resulting from rolling and yawing disturbances, calculations were made to determine the motions following a displacement in sideslip or bank of 5° for condition I. These motions are presented in figure 17. Here again the predominant motion is rolling regardless of whether the displacement was in yaw or roll.

CONCLUDING REMARKS

The following conclusions are based on the results of calculations of the lateral stability of Douglas design No. 39C, an early version of the X-3 research airplane.

1. The calculations indicated stability for the $M = 0.75$ condition and for the landing condition. The $M = 2.3$ condition could be made stable by increasing the vertical-tail area. Only the landing condition satisfied the Air Force requirement for satisfactory damping of the lateral oscillation.

2. The spiral mode for the $M = 0.75$ condition and the landing condition was slightly unstable but was well within the Air Force requirement.

3. The oscillatory stability was most sensitive to the damping-in-roll parameter and to the inclination of the principal axis of inertia.

4. Increasing the damping-in-roll parameter $-C_{l_p}$ increased the oscillatory stability for the landing condition but decreased the stability for the $M = 2.3$ condition. The decreased stability with increased damping in roll for the $M = 2.3$ condition is attributed to the positive value of the derivative C_{n_p} and to the negative inclination of the principal axis of inertia.

5. A disturbance in yaw or roll resulted in a predominantly rolling motion.

Langley Aeronautical Laboratory
National Advisory Committee For Aeronautics
Langley Field, Va.

REFERENCES

1. Douglas Aircraft Company: Subsonic Dynamic Lateral Stability of the MX-656 Airplane (Design No. 39C). Report No. SM-13196, 1948.

2. Douglas Aircraft Company: Supersonic Dynamic Lateral Stability of the MX-656 Airplane (Design No. 39C). Report No. SM-13061, 1947.

3. Sternfield, Leonard, and Gates, Ordway, B., Jr.: A Simplified Method for the Determination and Analysis of the Neutral-Lateral-Oscillatory-Stability Boundary. NACA TN No. 1727, 1948.

4. Routh, Edward John: Dynamics of a System of Rigid Bodies. Part II. Sixth ed., rev. and enl., Macmillan and Co. Ltd., 1905, p. 223.

5. Bennett, Charles V., and Hassell, James L., Jr.: Stability and Control Characteristics of a Free-Flying Model with an Unswept Wing of Aspect Ratio 3 (XS-3). NACA RM No. L8J04, 1948.

6. Toll, Thomas A., and Queijo, M. J.: Approximate Relations and Charts for Low-Speed Stability Derivatives of Swept Wings. NACA TN No. 1581, 1948.

7. Bamber, Millard J.: Effect of Some Present-Day Airplane Design Trends on Requirements for Lateral Stability. NACA TN No. 814, 1941.

8. Harmon, Sidney M.: Stability Derivatives of Thin Rectangular Wings at Supersonic Speeds. Wing Diagonals ahead of Tip Mach Lines. NACA TN No. 1706, 1948.

9. Sternfield, Leonard: Some Considerations of the Lateral Stability of High-Speed Aircraft. NACA TN No. 1282, 1947.

TABLE I

CHARACTERISTICS OF DOUGLAS DESIGN NO. 39C USED FOR CALCULATIONS

	Condition I	Condition II	Condition III
Mach number	0.75	2.3	0.206
Altitude, ft	35,000	35,000	0
Weight, lb	15,229	14,153	12,170
Wing loading, W/S	95.18	88.45	76.06
Glide path, γ, deg	0	0	0
Velocity, V, ft/sec	719.7	2205.86	230.26
Wing span, b, ft	21.92	21.92	21.92
Lift coefficient, C_L	0.50	0.05	1.2
μ	182.75	169.83	45.32
ρ	0.000738	0.000738	0.002378
Angle of attack, α, deg	8	0	13
ϵ, deg	2	2	2
η, deg	6	-2	11
l/b	0.91	0.91	0.91
z/b	0.264	0.264	0.264
k_{X_o}, ft	2.9	2.9	2.9
k_{Z_o}, ft	12.0	12.0	12.0
C_{l_p}	$-0.27 - 2.37C_{n_\beta}$	$-0.25 - 8.54C_{n_\beta}$	$-0.27 - 0.45C_{n_\beta}$
C_{l_r}	$0.125 + 17.27C_{n_\beta}$	$-0.00138 + 30.254C_{n_\beta}$	$0.30 + 6.88C_{n_\beta}$
C_{n_r}	$-0.005 - 104.29C_{n_\beta}$	$0.000203 - 104.29C_{n_\beta}$	$-0.10 - 104.29C_{n_\beta}$
C_{n_p}	$0.05 + 17.27C_{n_\beta}$	$0 + 30.254C_{n_\beta}$	$-0.10 + 6.88C_{n_\beta}$
C_{n_β} (tail off)	0	0	0
C_{Y_β}	$-0.248 - 63.03C_{n_\beta}$	$-0.248 - 63.03C_{n_\beta}$	$-0.248 - 63.03C_{n_\beta}$
K_X^2	0.0206	0.0178	0.0299
K_Z^2	0.297	0.2996	0.259
K_{XZ}	0.0293	-0.0098	0.0529
$C_L \tan \gamma$	0	0	0
$C_{Y_p} = C_{Y_r}$	0	0	0

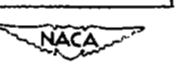

TABLE II

PERIOD AND TIME TO DAMP TO ONE-HALF AMPLITUDE

Airplane condition	C_L	M	Altitude (feet)	C_{n_β}	C_{l_β}	Oscillatory mode			Aperiodic mode	
						Period (sec)	$T_{1/2}$	$C_{1/2}$	$T_{1/2}$	$T_{1/2}$
I	0.5	0.75	35,000	0.006	-0.002	2.64	3.16	1.20	1.258	-304.2
II	.05	2.3	35,000	.0022	-.0014	2.04	-5.24	-2.57	.2526	141.7
[a]II	.05	2.3	35,000	.0047	-.0024	1.40	8.39	6.00	2.647	99.0
III	1.2	.206	0	.0096	-.00275	2.85	2.45	.86	.841	-64.1

[a]Signifies the airplane equipped with vertical tail area of 35 sq ft instead of the design tail of 25 sq ft.

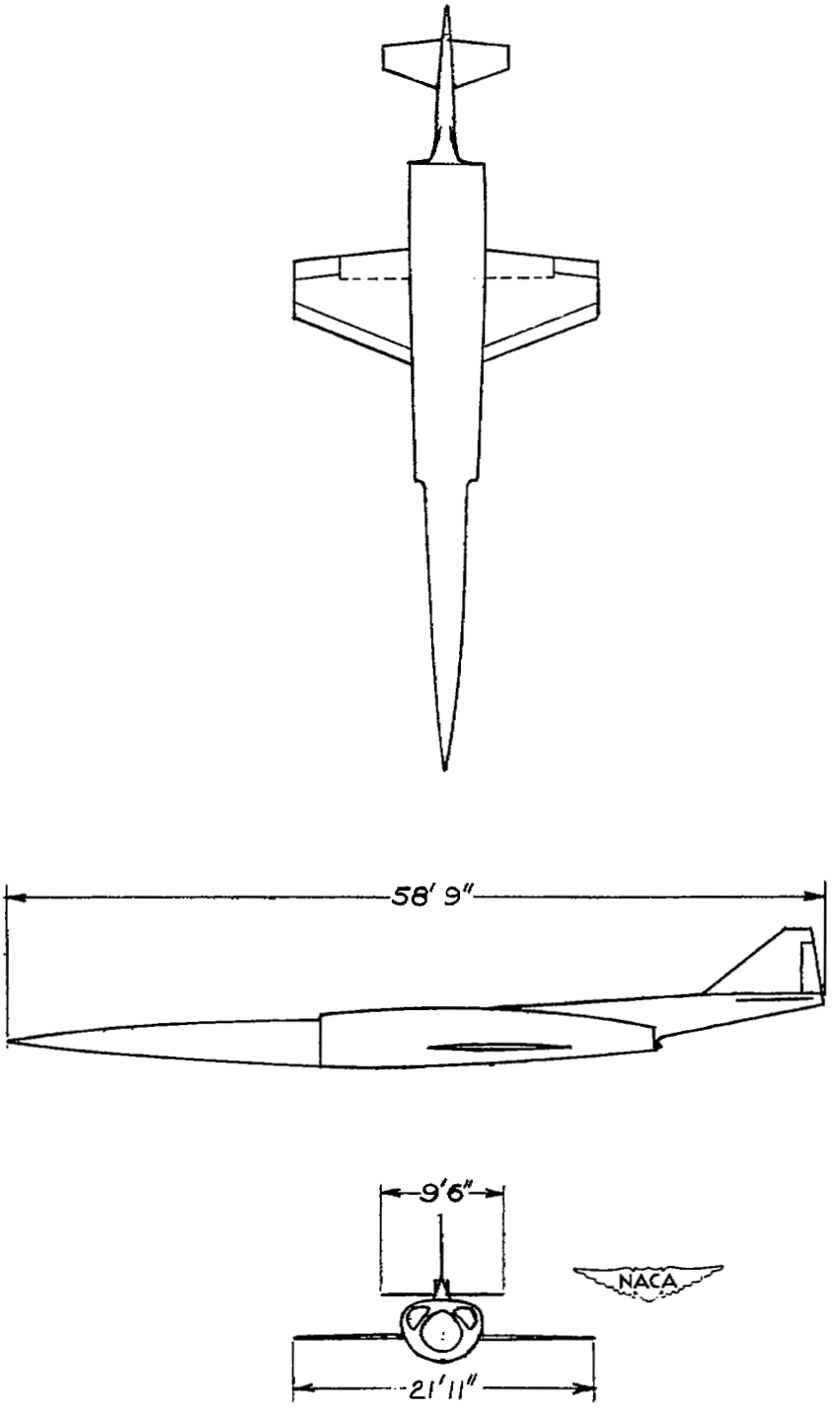

Figure 1.- Three-view sketch of Douglas design No. 39C, an early version of the X-3 research airplane.

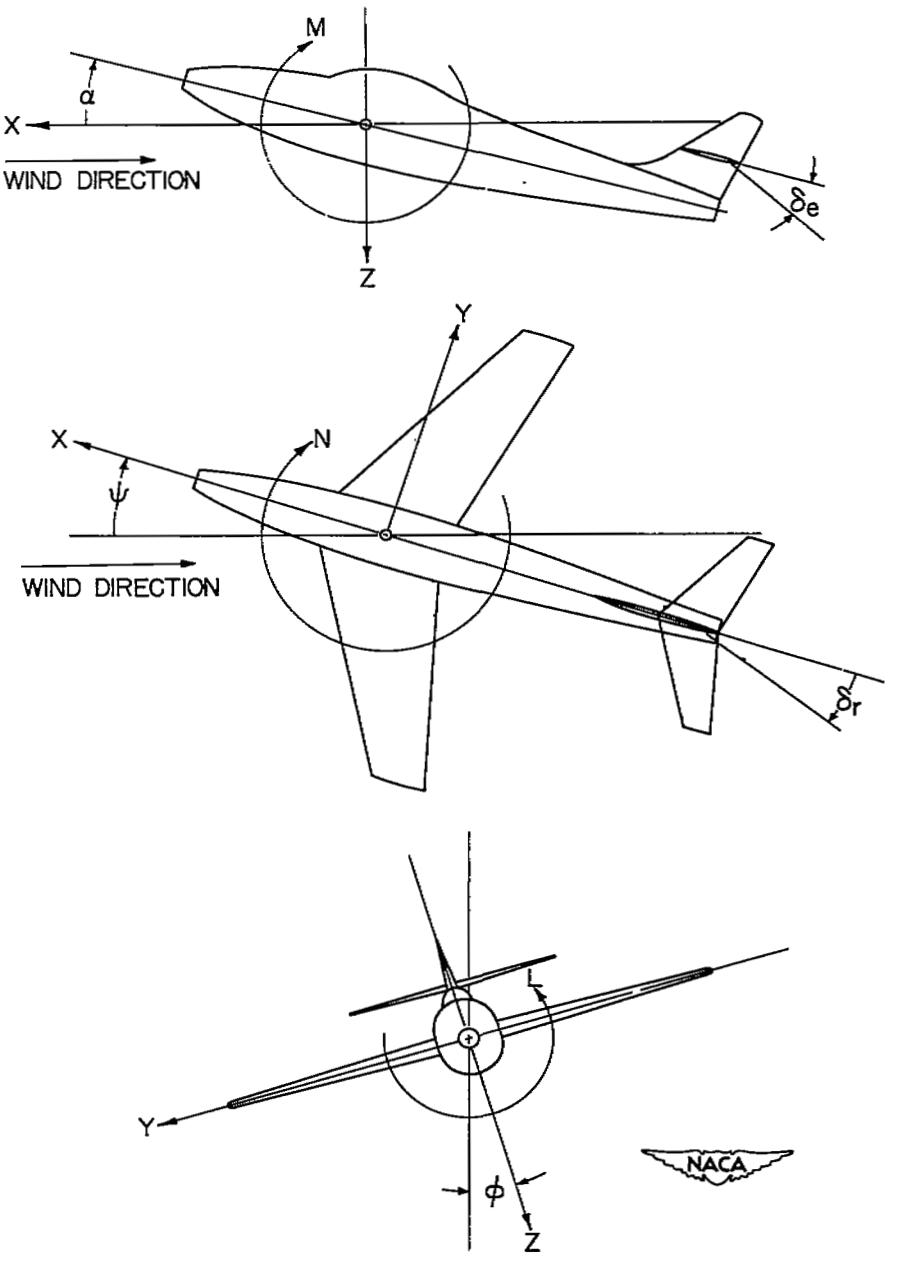

Figure 2.- The stability system of axes. Arrows indicate positive directions of moments, forces, and control-surface deflections. This system of axes is defined as an orthogonal system having their origin at the center of gravity and in which the Z-axis is in the plane of symmetry and perpendicular to the relative wind, the X-axis is in the plane of symmetry and perpendicular to the Z-axis, and the Y-axis is perpendicular to the plane of symmetry.

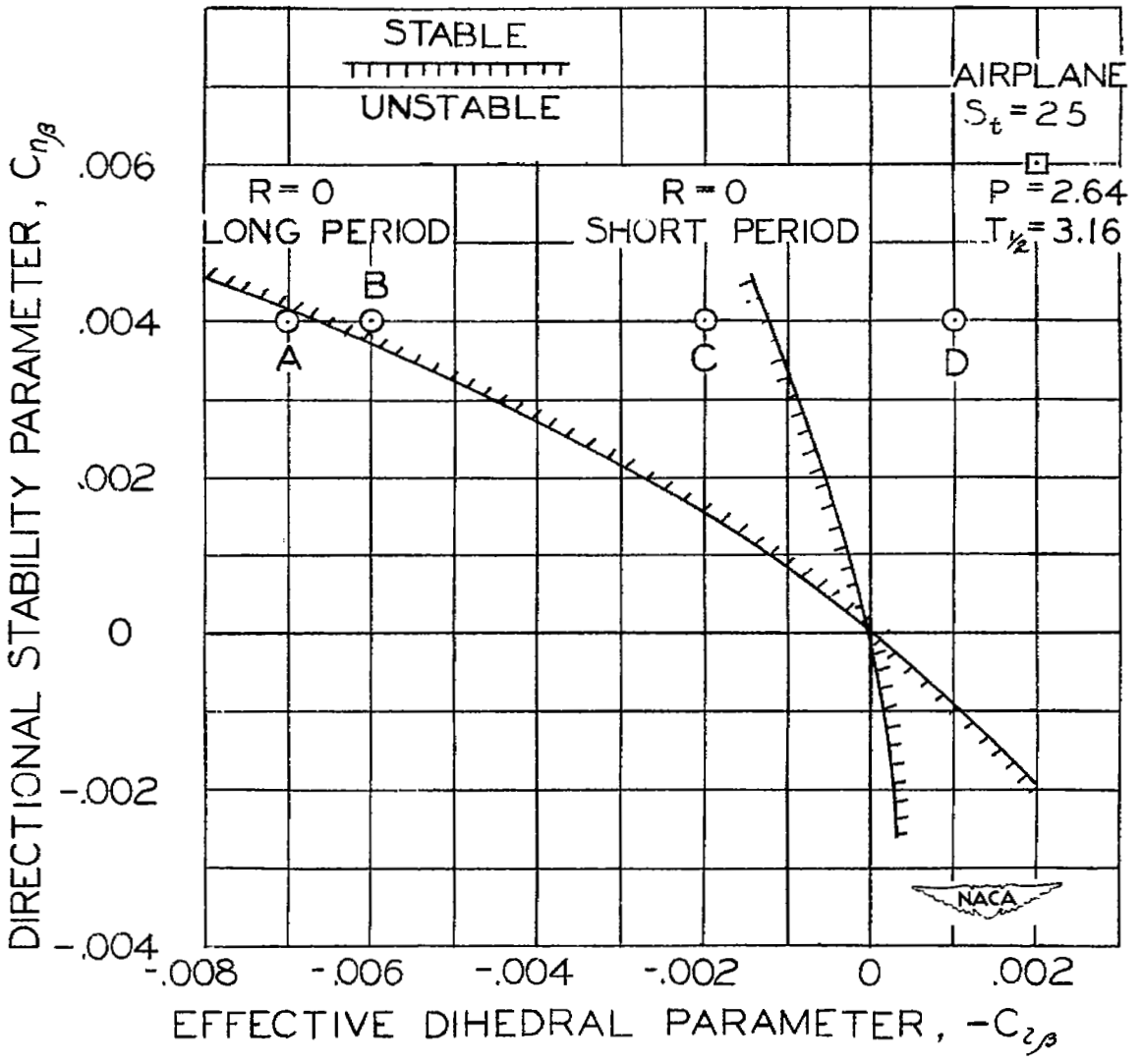

Figure 3.- Oscillatory-stability boundary as calculated for Douglas design No. 39C. Flight condition I (M = 0.75; C_L = 0.50; altitude, 35,000 ft).

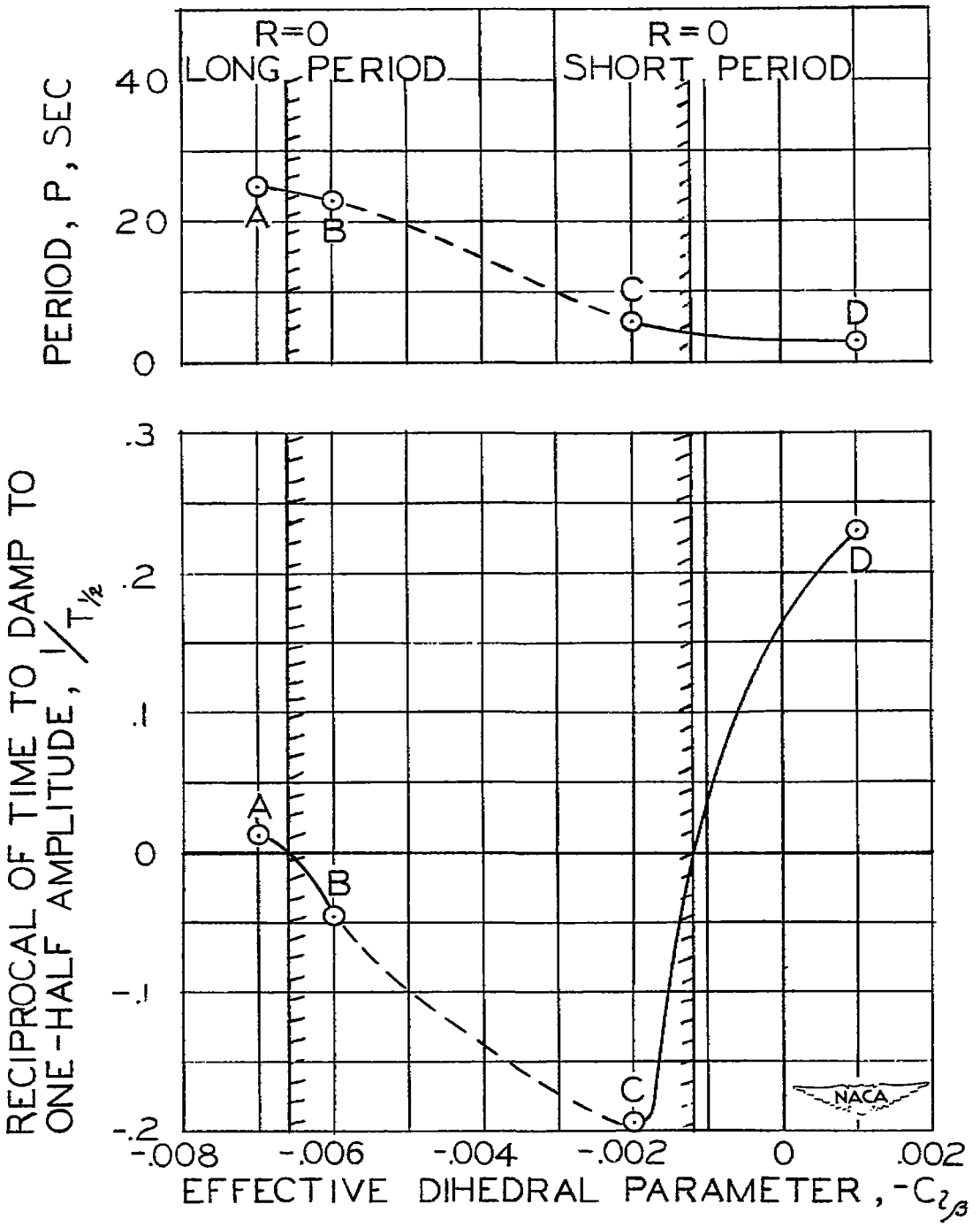

Figure 4.- Effect on period and time to damp to one-half amplitude of crossing oscillatory-stability boundary for Douglas design No. 39C. Flight condition I.

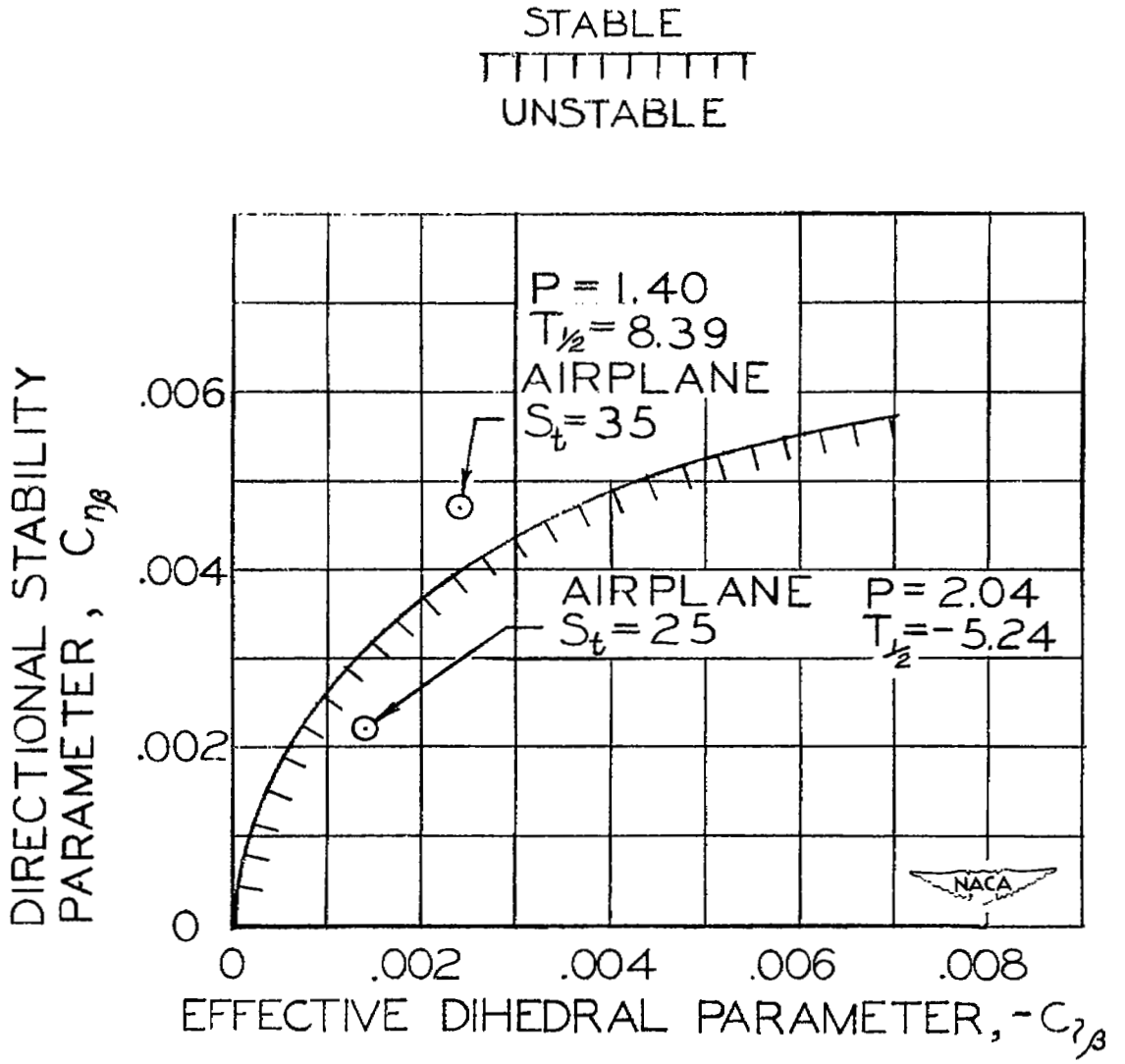

Figure 5.- Oscillatory-stability boundary as calculated for Douglas design No. 39C. Flight condition II (M = 2.3; C_L = 0.05; altitude, 35,000 ft).

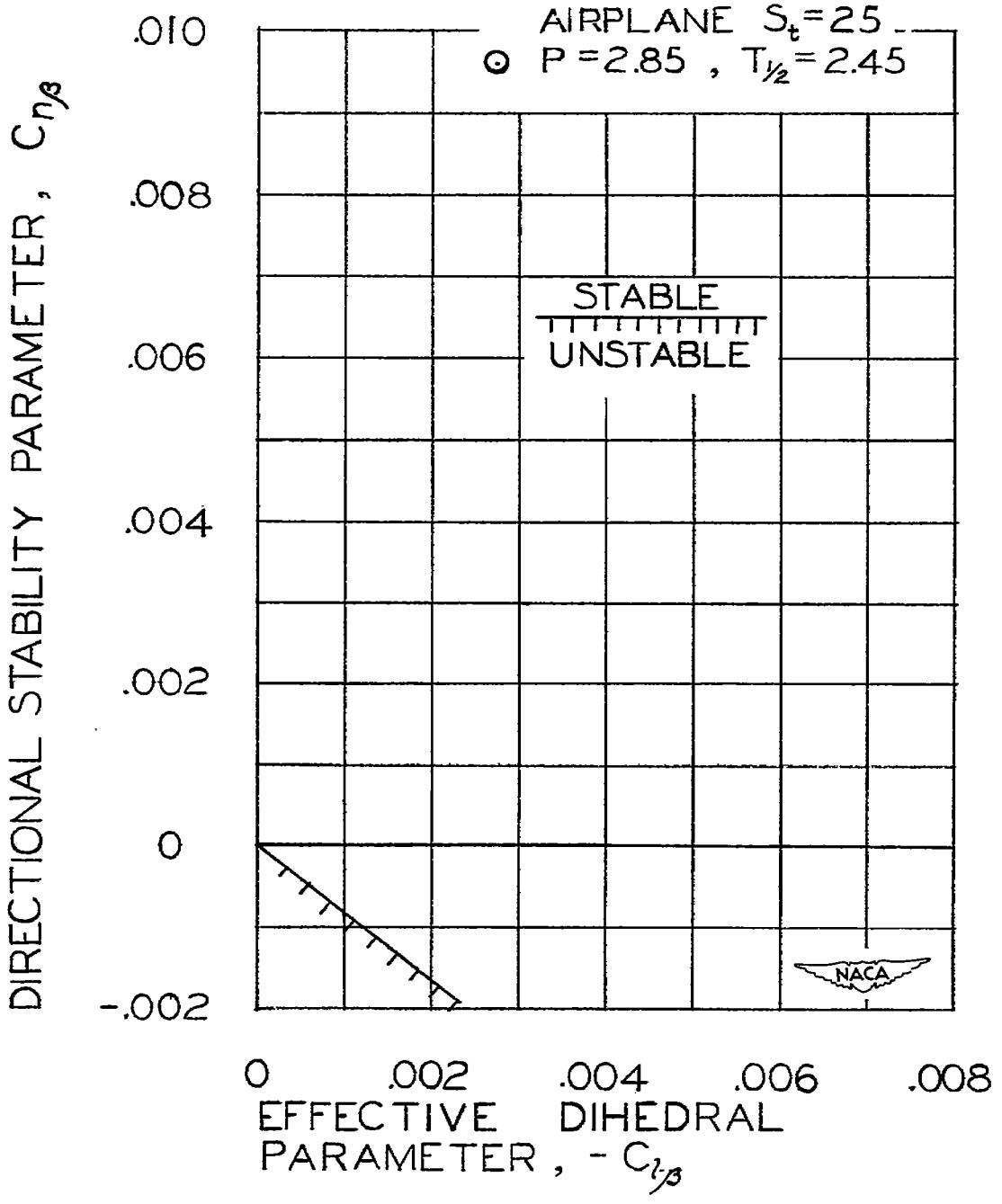

Figure 6.- Oscillatory-stability boundary as calculated for Douglas design No. 39C. Flight condition III (M = 0.206; C_L = 1.2; altitude, sea level).

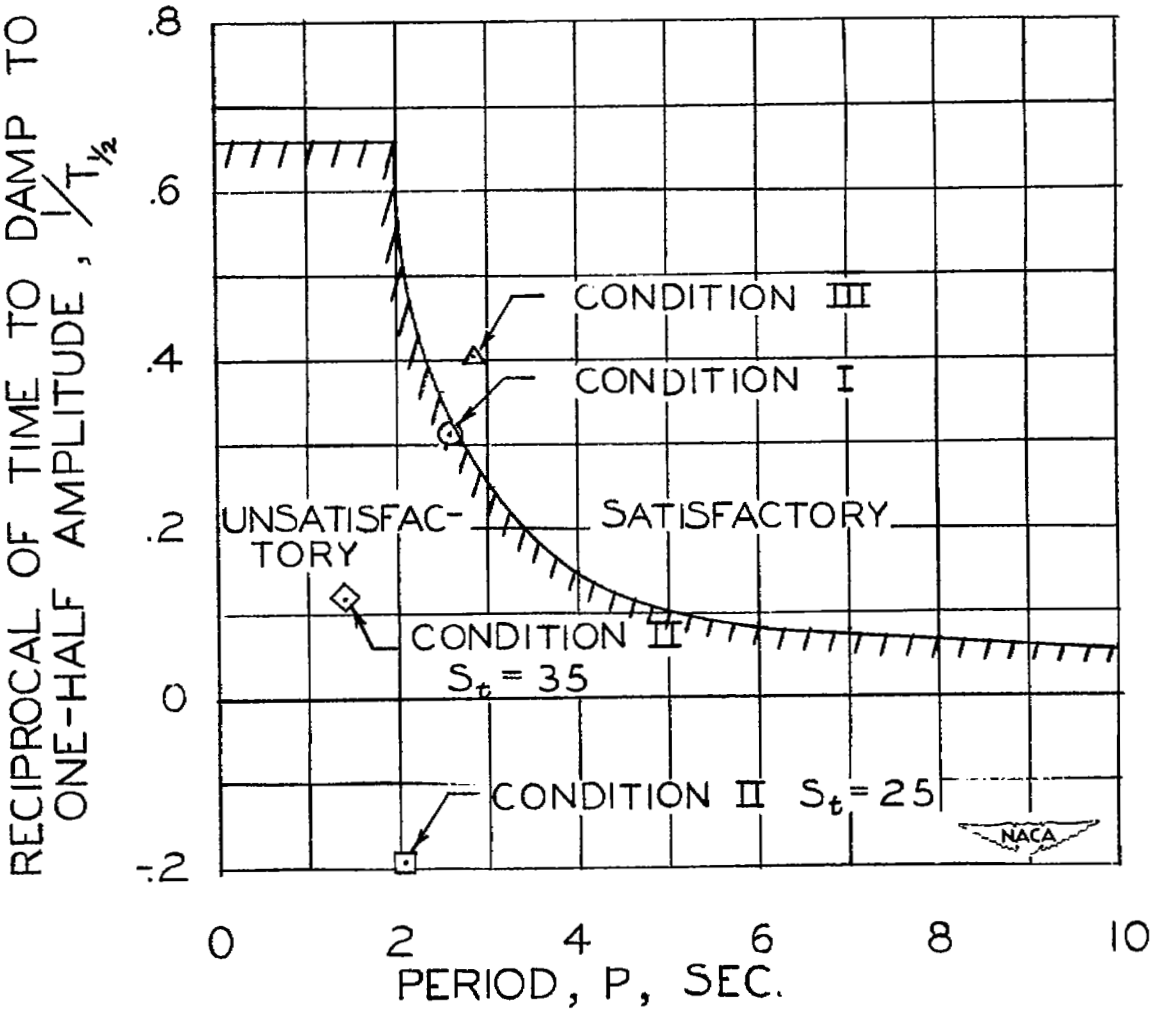

Figure 7.- Calculated damping of Douglas design No. 39C as compared with the Air Force requirements for satisfactory damping of the lateral oscillation.

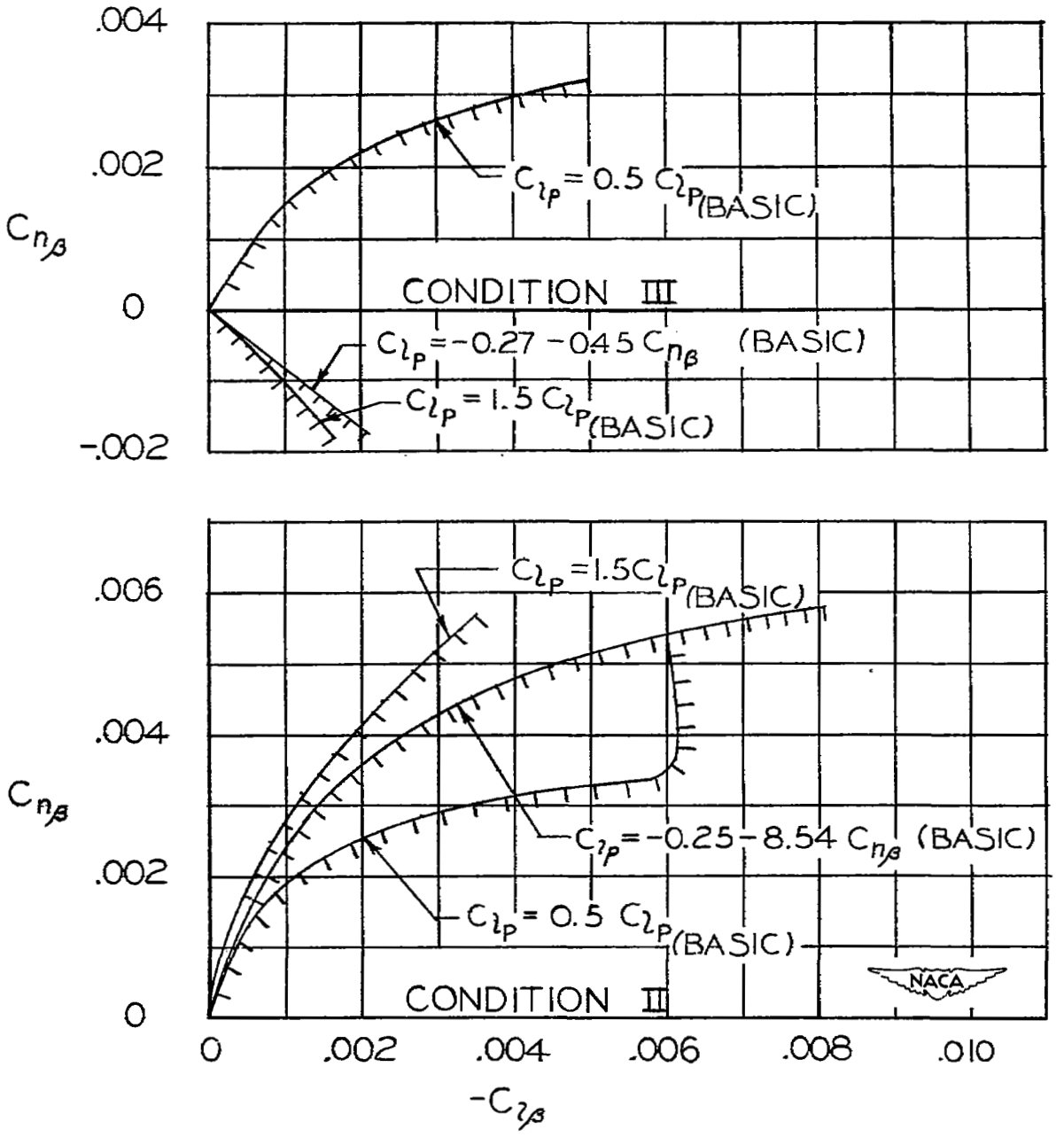

Figure 8.- Effect on the R = 0 boundary of increasing or decreasing C_{l_p} by 50 percent for flight conditions II and III.

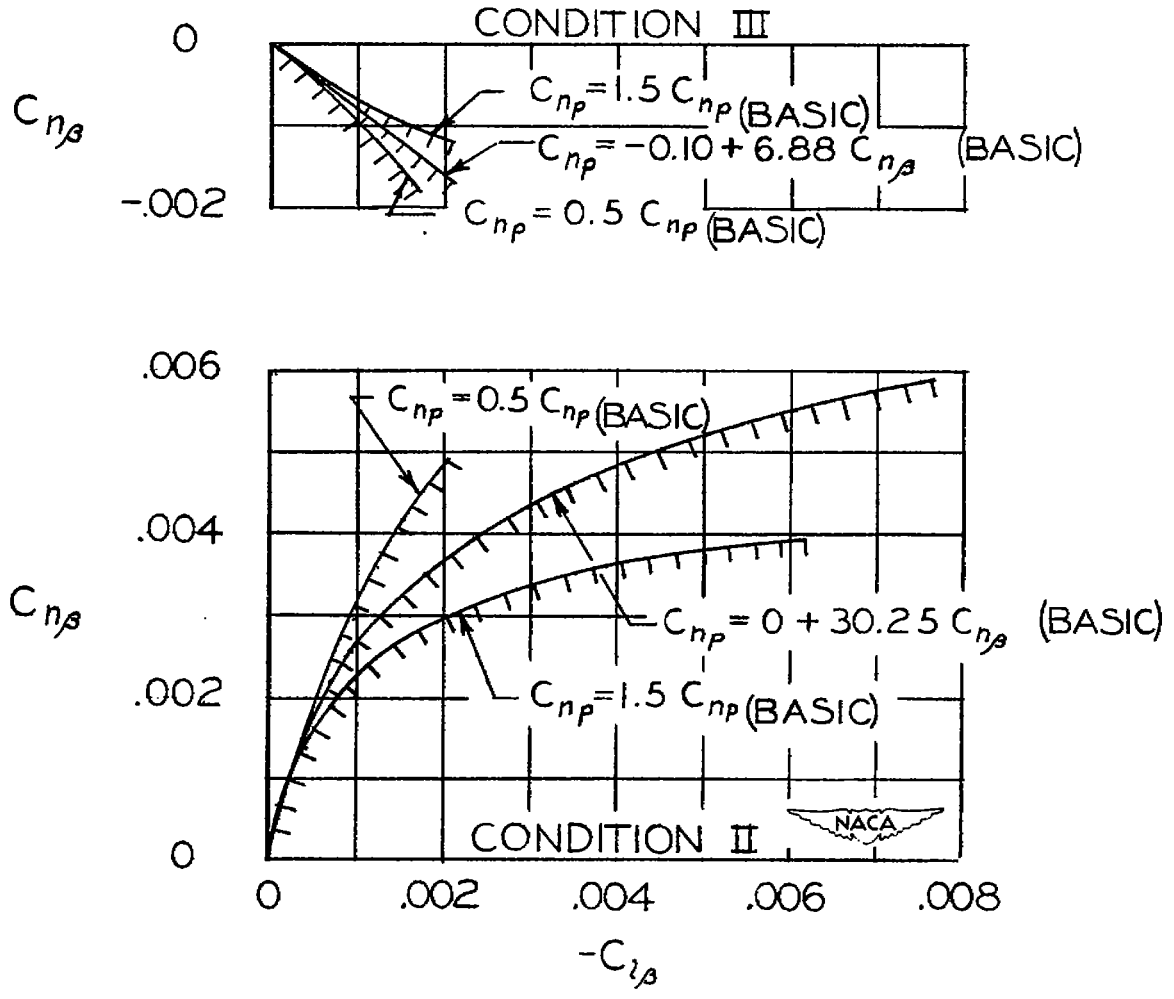

Figure 9.- Effect on the R = 0 boundary of increasing or decreasing C_{n_p} by 50 percent for flight conditions II and III.

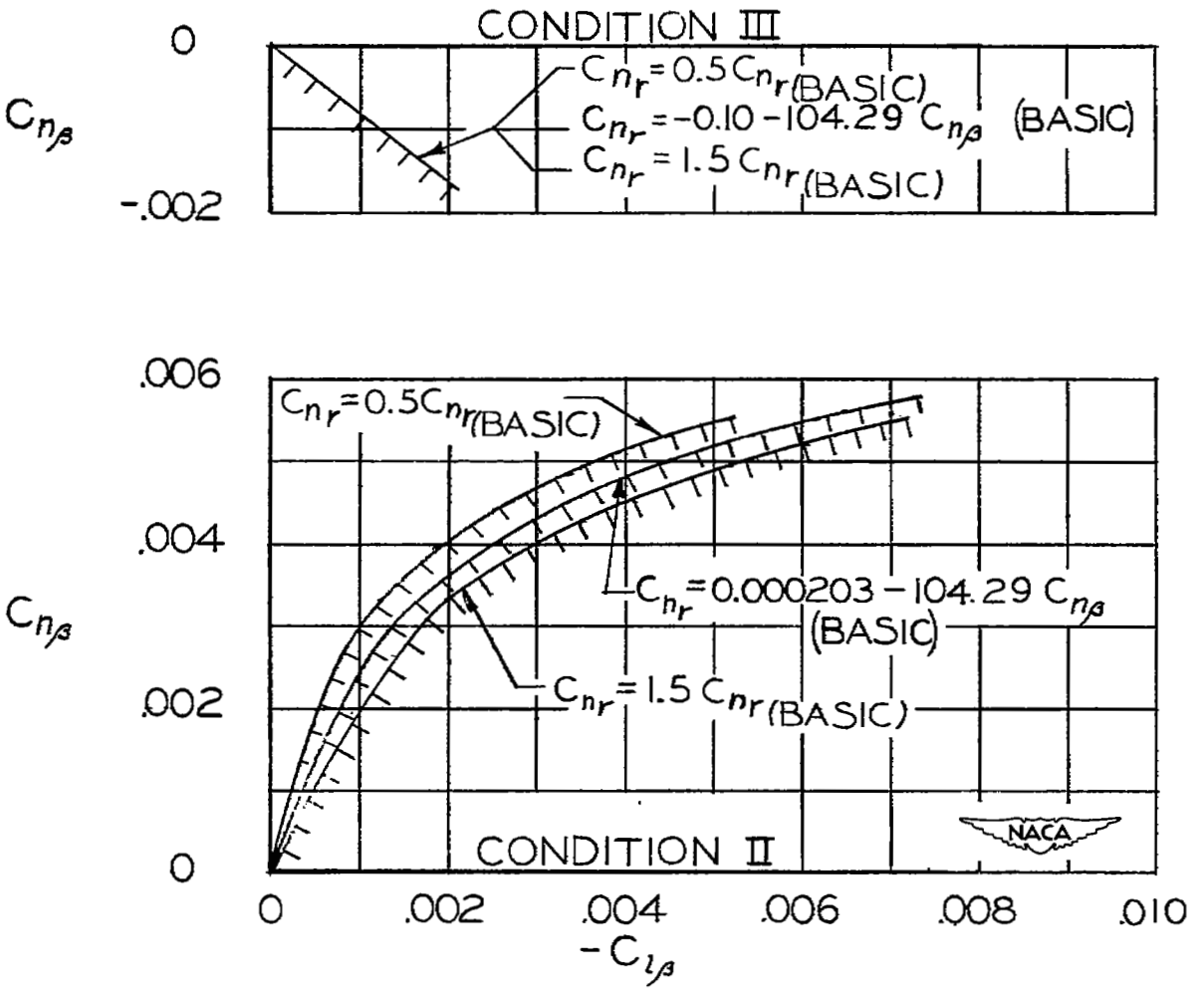

Figure 10.- Effect on the R = 0 boundary of increasing or decreasing C_{n_r} by 50 percent for flight conditions II and III.

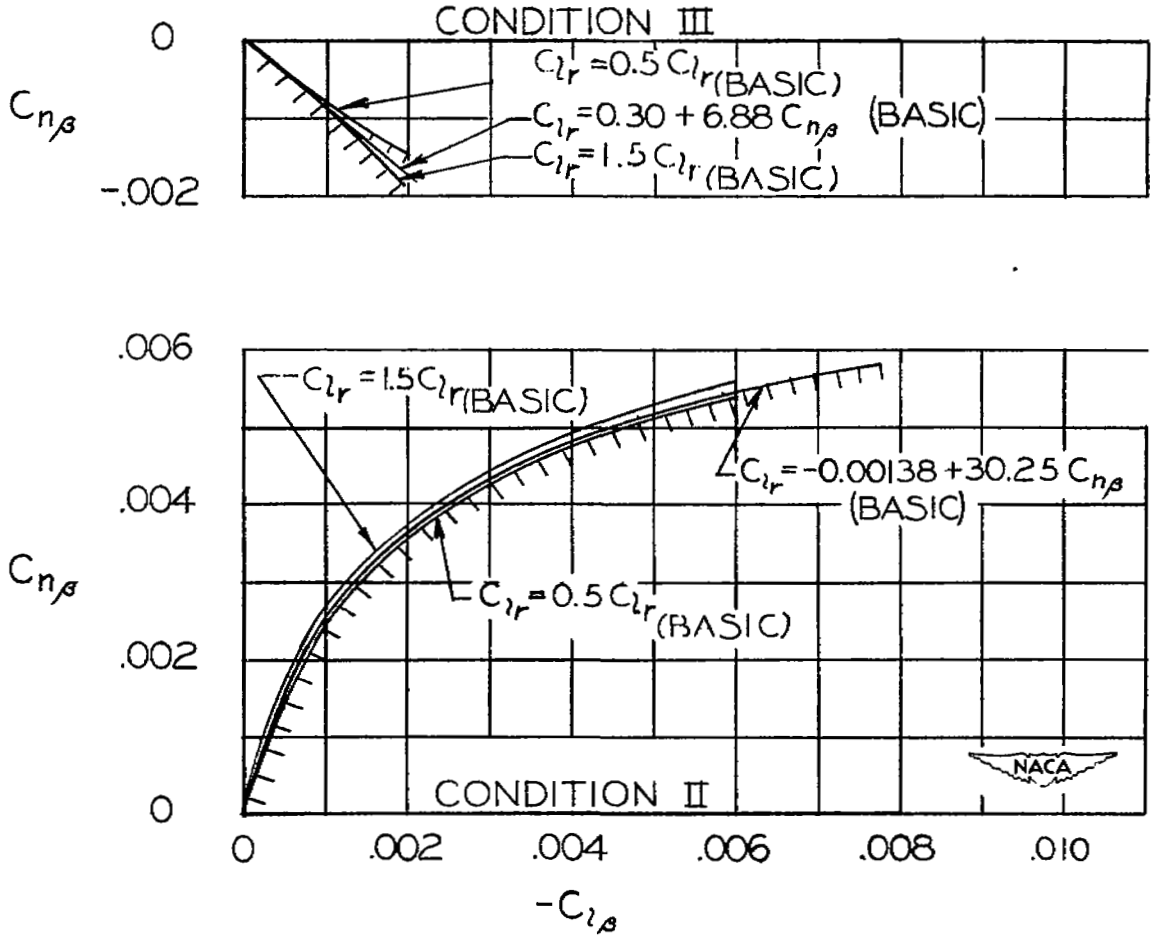

Figure 11.- Effect on the R = 0 boundary of increasing or decreasing C_{l_r} by 50 percent for flight conditions II and III.

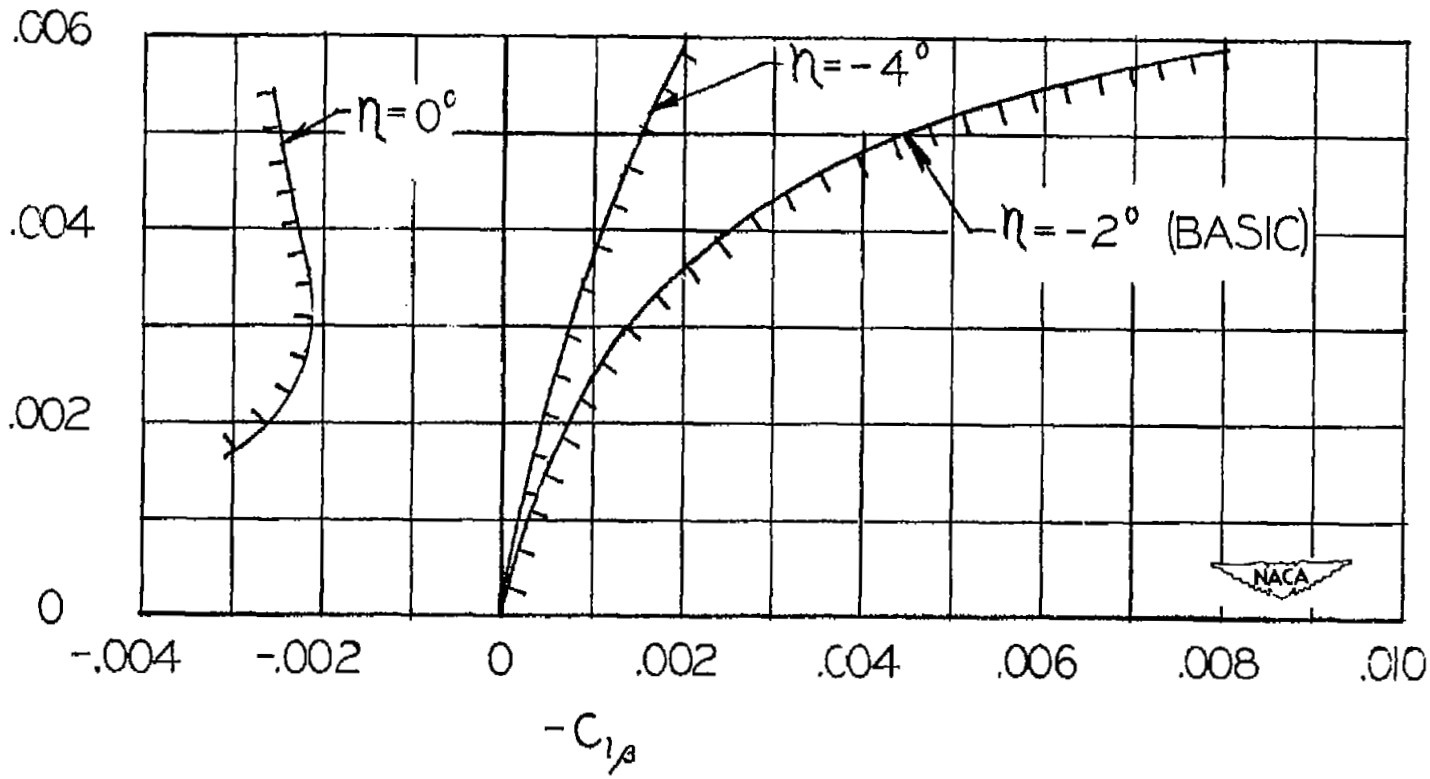

Figure 12.- Effect on the R = 0 boundary of increasing or decreasing η for condition II.

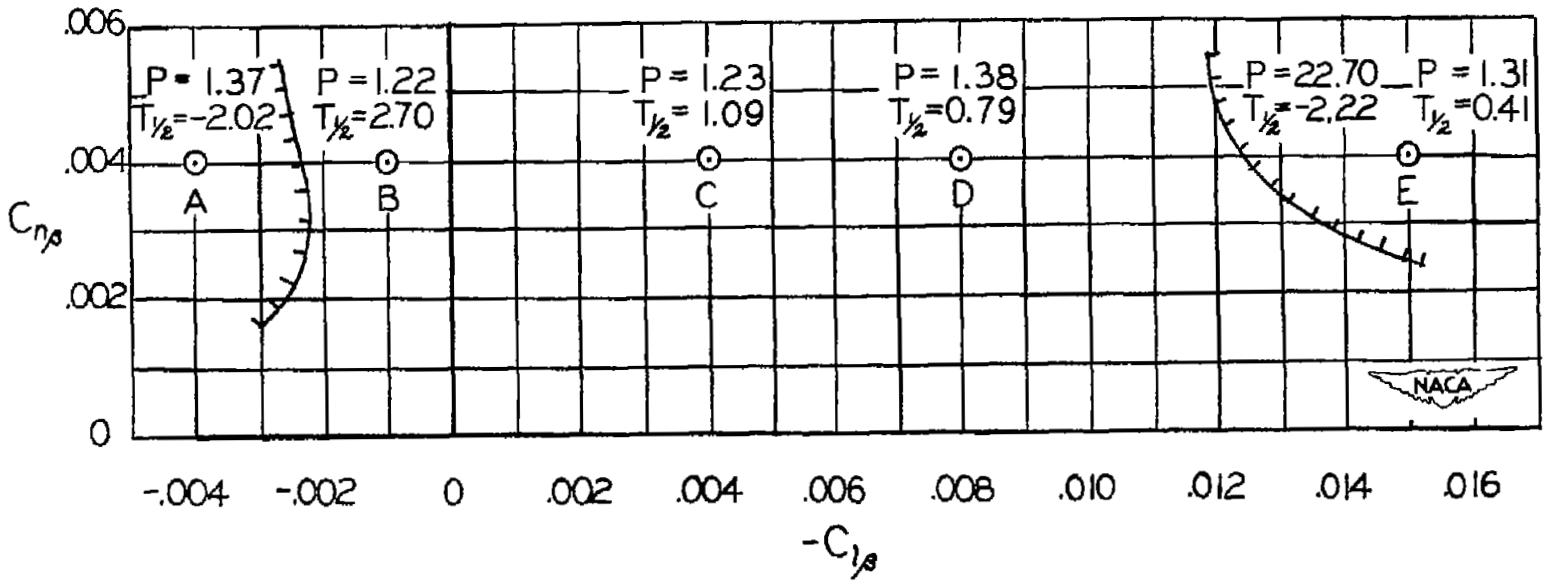

Figure 13.- Effect on the period and time to damp of crossing the R = 0 boundary for condition II. $\eta = 0^\circ$.

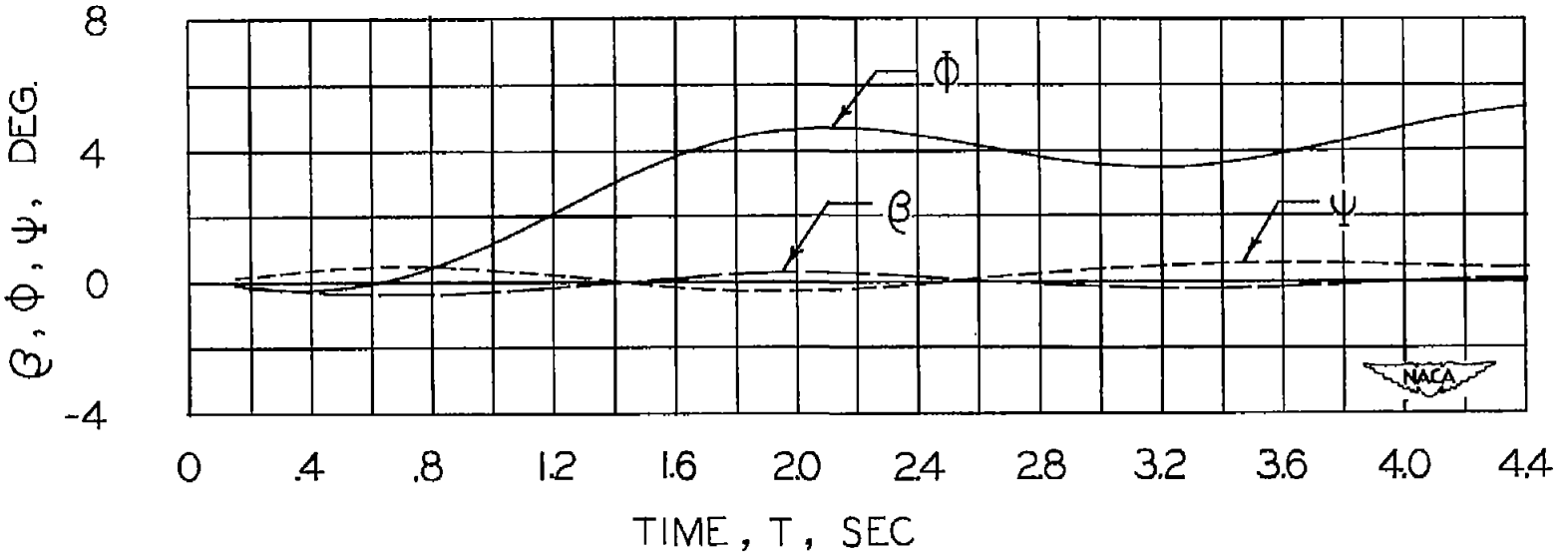

(a) Yaw disturbance.

Figure 14.- Motion of Douglas design No. 39C resulting from a disturbance in yaw or roll. Condition I.

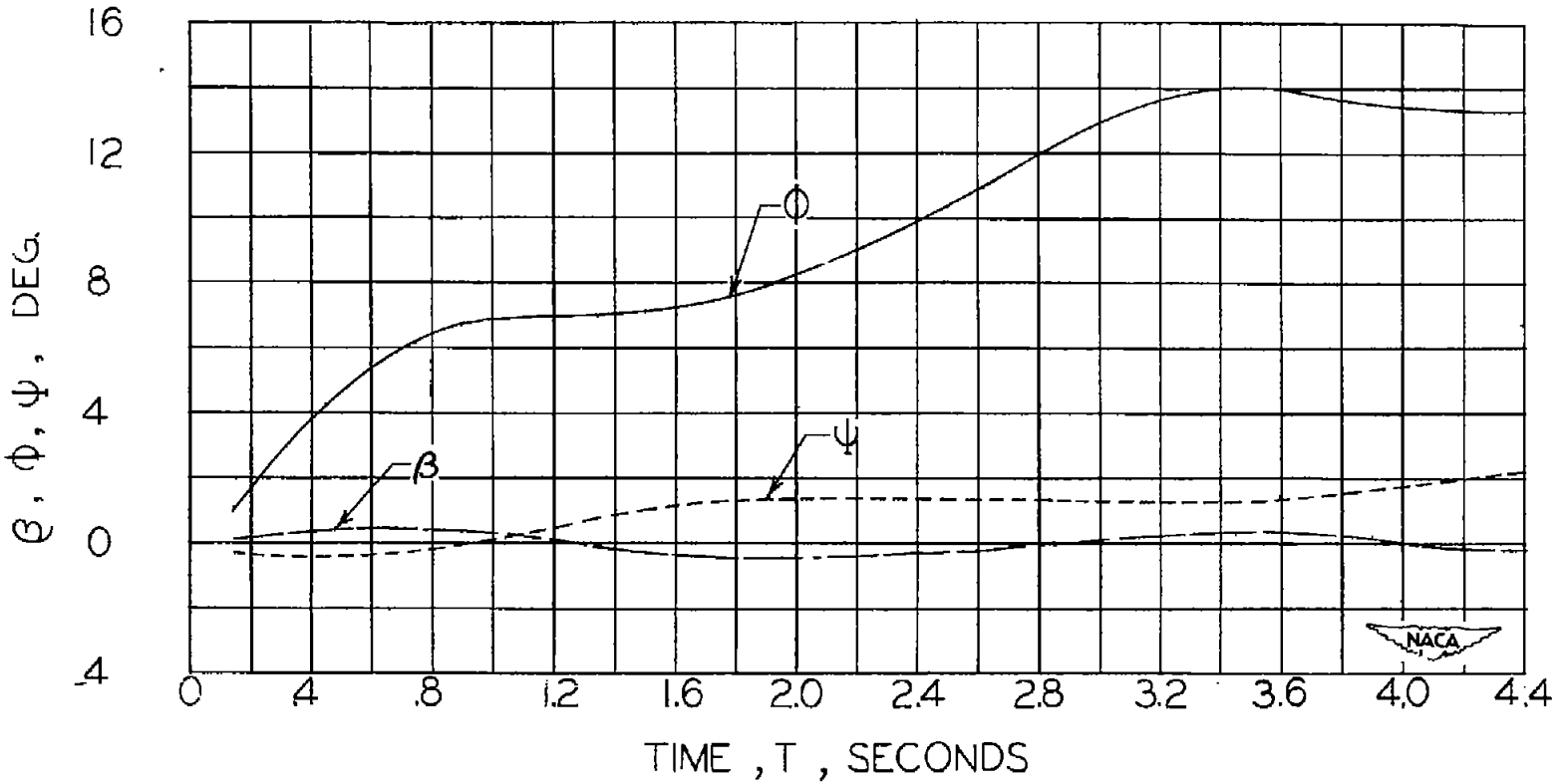

(b) Roll disturbance.

Figure 14.- Concluded.

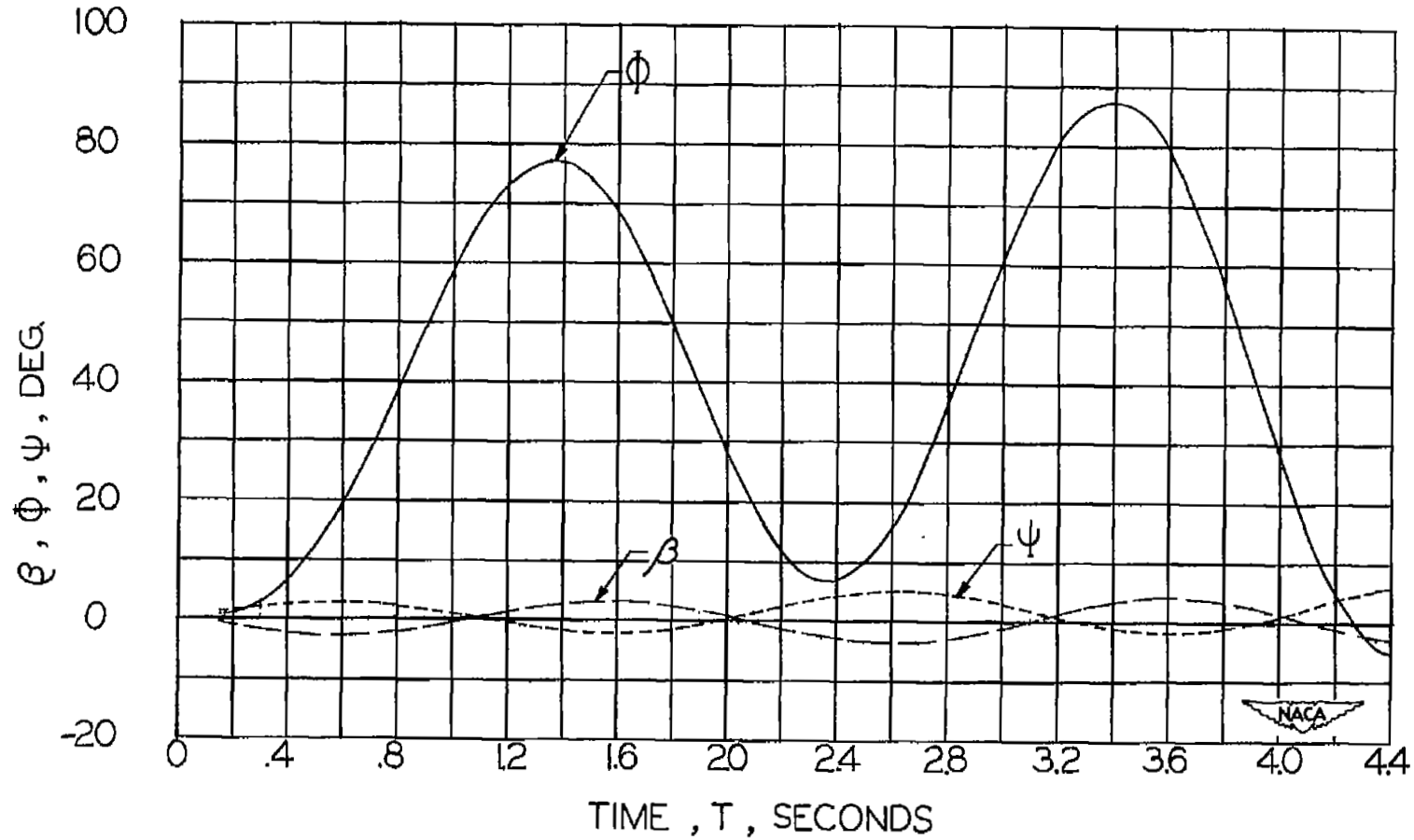

(a) Yaw disturbance. S_t = 25 sq ft.

Figure 15.- Motion of Douglas design No. 39C resulting from a disturbance in yaw or roll. Condition II.

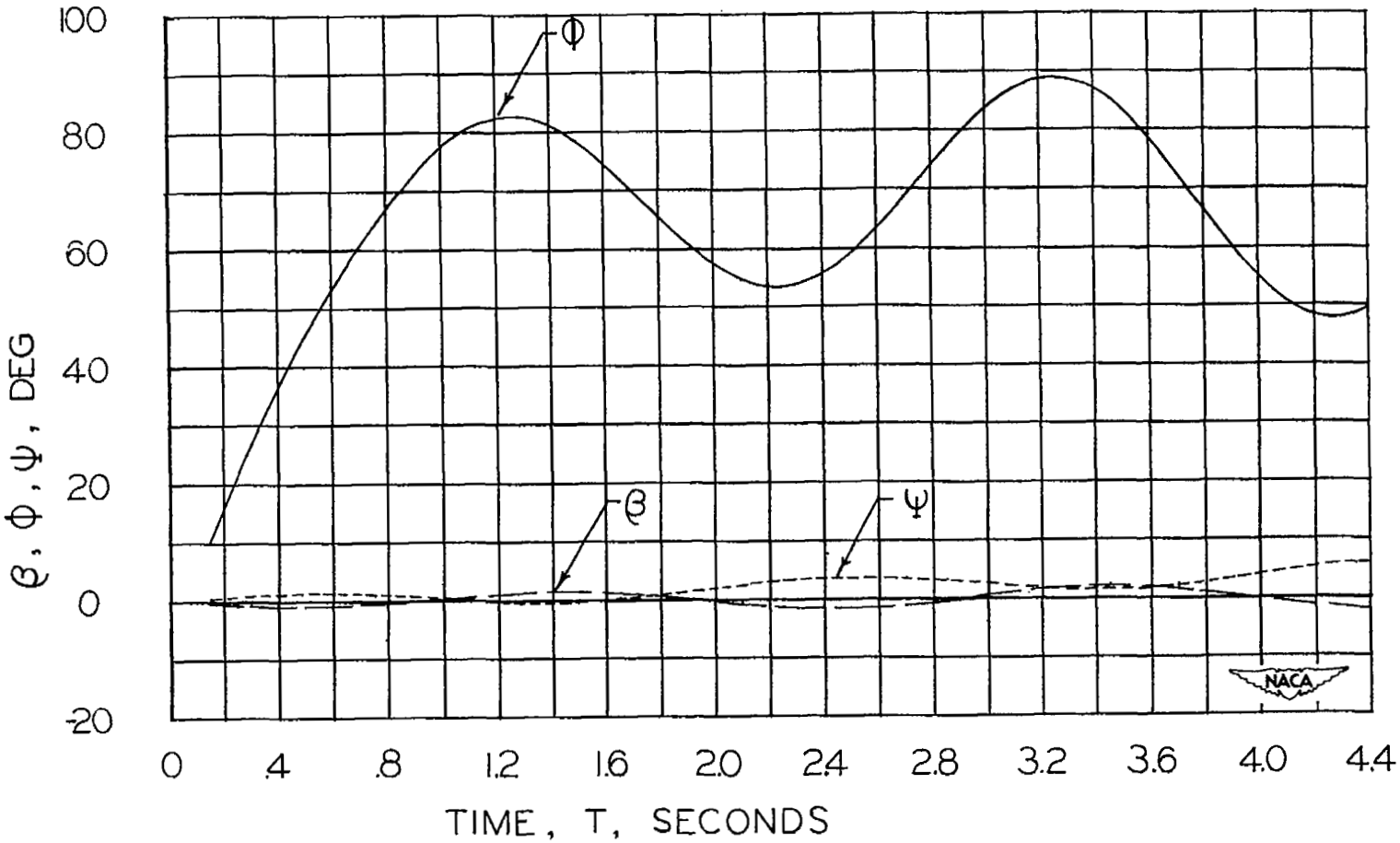

(b) Roll disturbance. S_t = 25 sq ft.

Figure 15.- Continued.

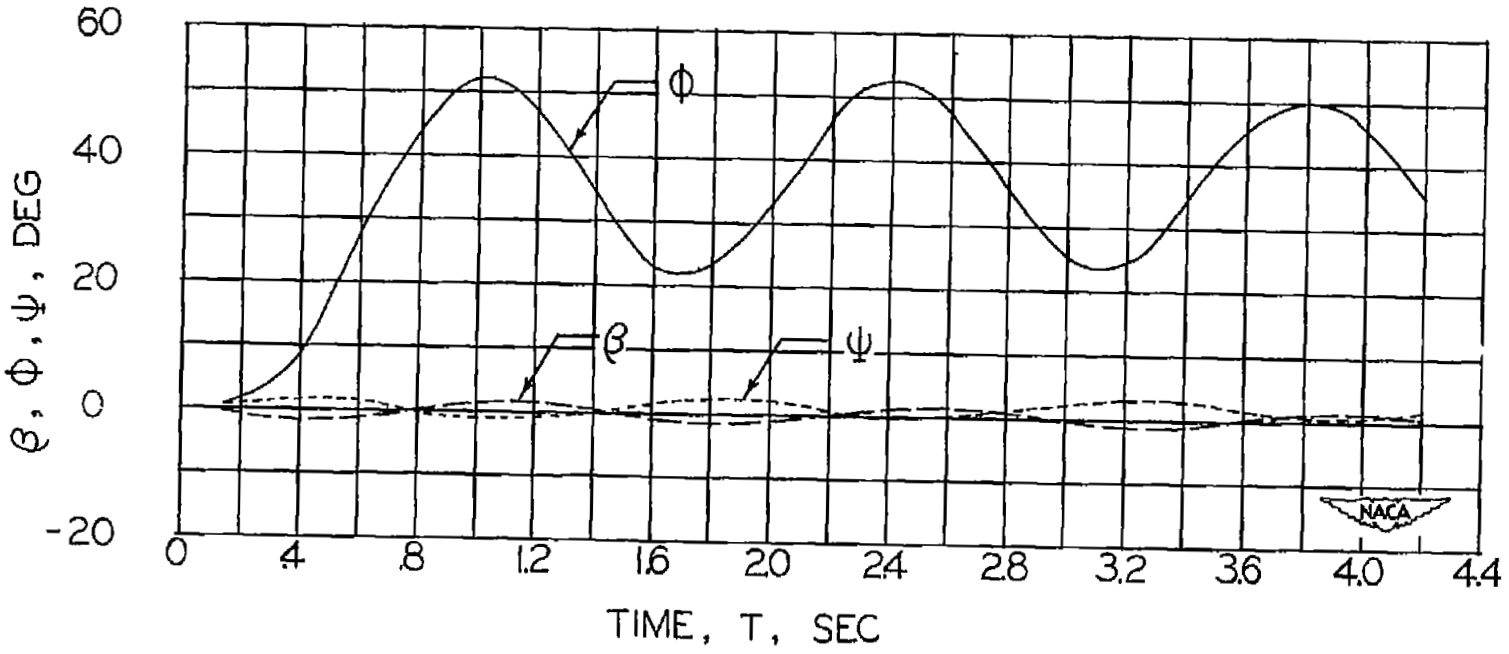

(c) Yaw disturbance. S_t = 35 sq ft.

Figure 15.- Continued.

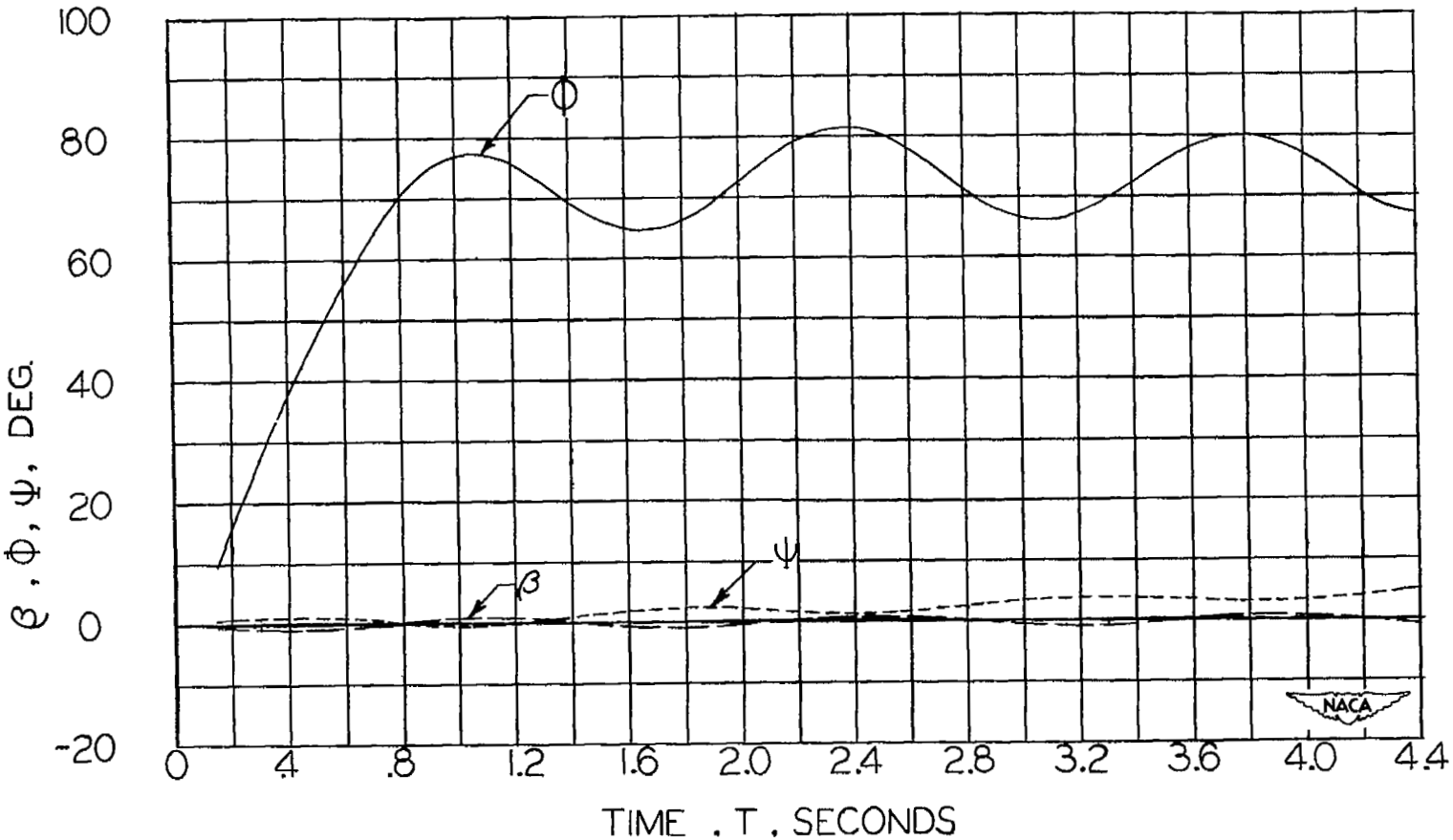

(d) Roll disturbance. S_t = 35 sq ft.

Figure 15.- Concluded.

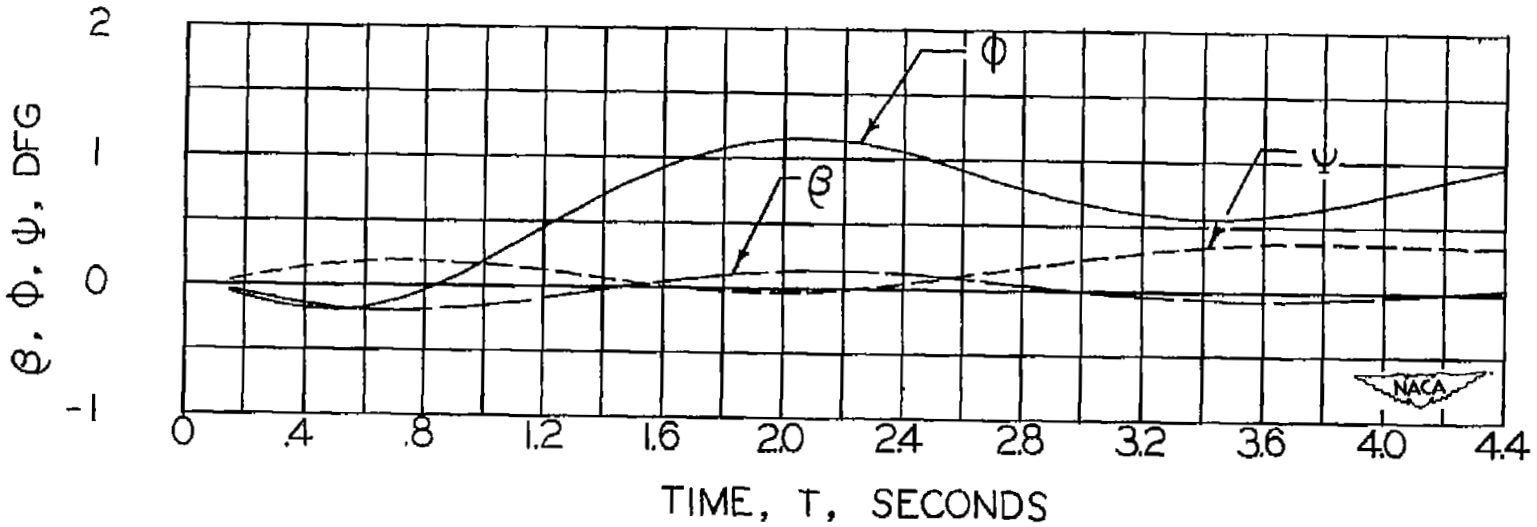

(a) Yaw disturbance.

Figure 16.- Motion of Douglas design No. 390 resulting from a disturbance in yaw or roll. Condition III.

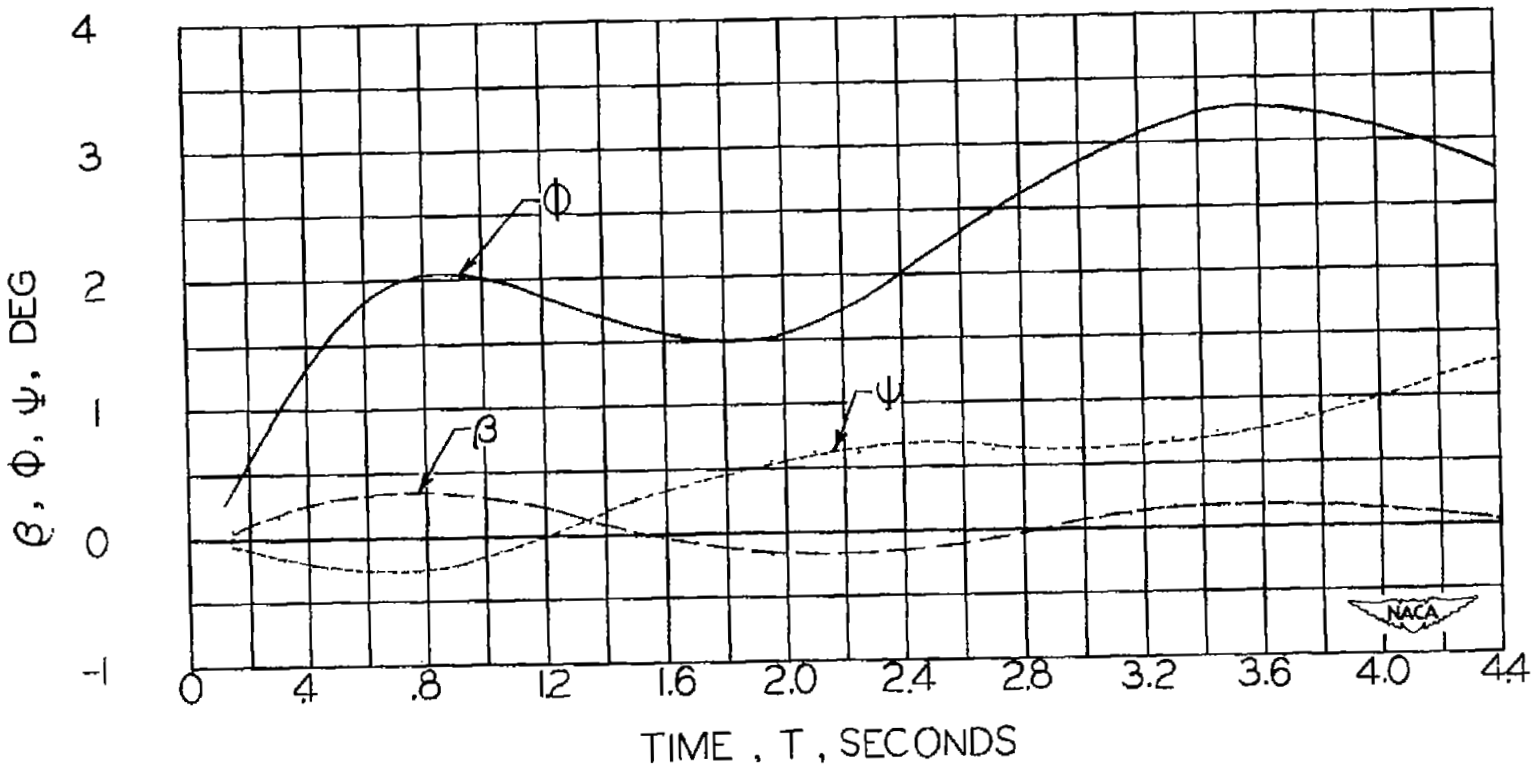

(b) Roll disturbance.

Figure 16.- Concluded

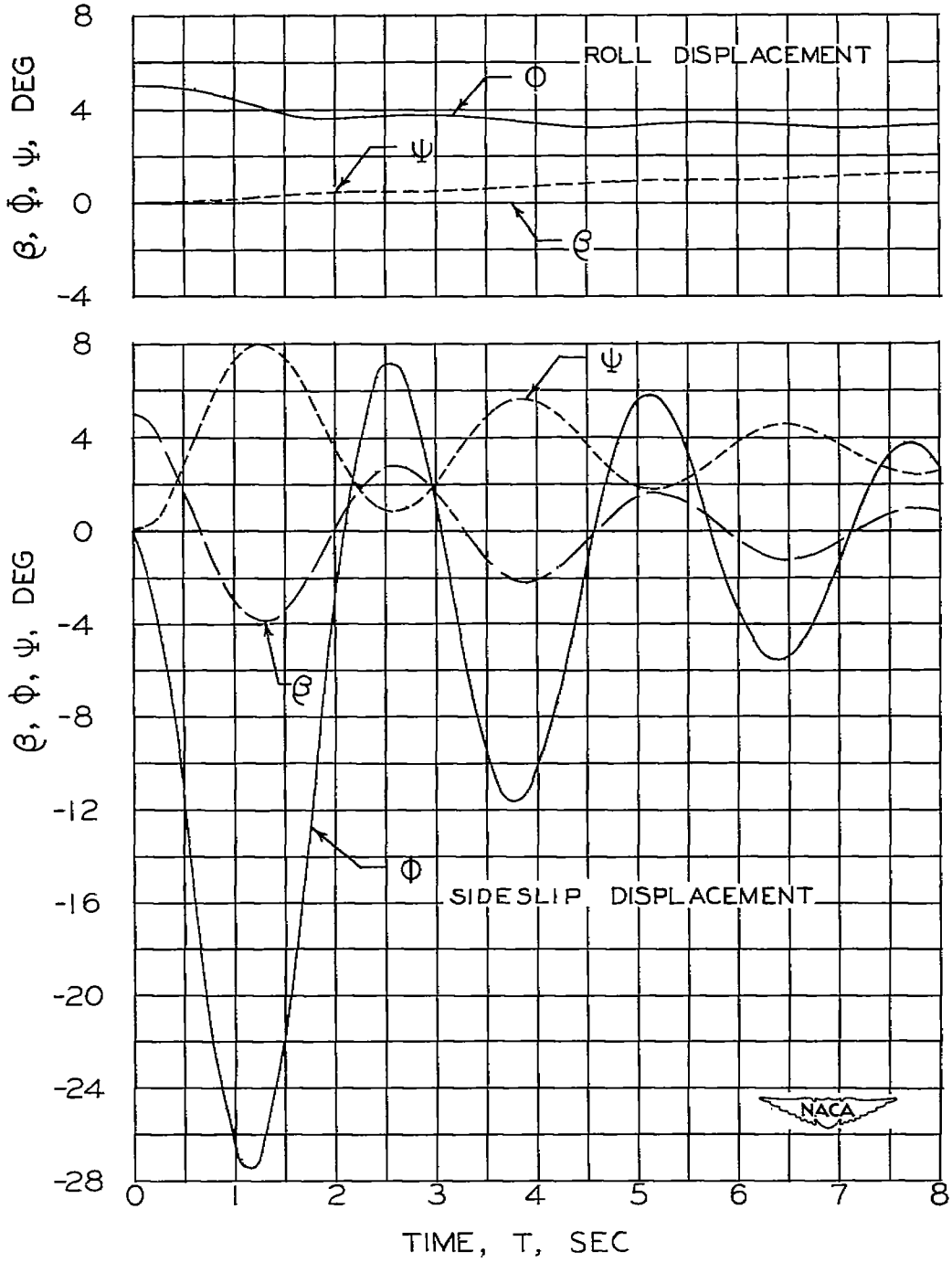

Figure 17.- Motion of Douglas design No. 39C resulting from a displacement in sideslip or roll of 5°. Condition I.